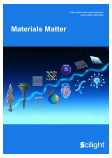
Scilight

Materials Matter

https://www.sciltp.com/journals/mm



Article

Multi-Stress Coupling Aging of Silicon Heterojunction Modules: Encapsulant Degradation and Reliability Implications

Hong Luo [1], Yu Hu [2,*], Qi Deng [1], Xiaoying Ye [1], Yulin Zhang [2], Cheng Huang [1], Tao Chen [3], Lei Li [4], Wenzhu Liu [5,*] and Jian Yu [1,*]

[1] School of New Energy and Materials, Southwest Petroleum University, Chengdu 610500, China
[2] Leshan West Silicon Materials Photovoltaic and New Energy Industry Technology Research Institute, Leshan 614000, China
[3] State Key Laboratory of Silicon and Advanced Semiconductor Materials, Zhejiang University, Hangzhou, 310027, China
[4] School of Physics and Electronical Science, Chuxiong Normal University, Chuxiong 675000, China
[5] Shanghai Institute of Microsystem and Information Technology, Chinese Academy of Sciences, Shanghai 201800, China
* Correspondence: huyu82@lsnu.edu.cn (Y.H.); wenzhu.Liu@mail.sim.ac.cn (W.L.); jianyu@swpu.edu.cn (J.Y.)

How To Cite: Luo, H.; Hu, Y.; Deng, Q.; et al. Multi-Stress Coupling Aging of Silicon Heterojunction Modules: Encapsulant Degradation and Reliability Implications. *Materials Matter* **2026**, *1*(1), 4.

Received: 8 May 2026
Revised: 7 June 2026
Accepted: 12 June 2026
Published: 17 July 2026

Abstract: The long-term reliability of silicon heterojunction (SHJ) photovoltaic modules is pivotal for their outdoor deployment and commercial viability. However, prevailing reliability assessments often rely on single-factor aging tests, which inadequately represent the synergistic stresses encountered in real-world climates. This study emphasizes the critical necessity of multi-stress coupling aging for a true durability evaluation. We conducted comparative 1000-h aging tests on SHJ modules and three types of encapsulants (EVA, dsEVA, and POE) under both damp-heat (DH) and UV-damp-heat (UVDH) coupling conditions. The results demonstrated that degradation mechanisms and severity are profoundly amplified under coupled stresses. Under UVDH, massive moisture ingress caused deacetylation in EVA/dsEVA, generating acetic acid that corroded solar cells, solder ribbons, and electrodes. Conversely, POE films suffered a severe loss of interfacial adhesion, leading to pronounced delamination. A systematic analysis of optical, mechanical, and chemical property changes in the films revealed a direct correlation between encapsulant degradation and module performance loss. Critically, the degradation under UVDH coupling conditions was significantly more severe than under DH alone, highlighting the synergistic acceleration effect of combined ultraviolet radiation and humidity. This work conclusively shows that multi-stress coupling tests are imperative for an accurate reliability assessment. It is recommended to integrate such coupled-aging protocols into standard testing regimes to better predict module lifetime, guide encapsulant material optimization, and ensure sustainable field performance.

Keywords: silicon heterojunction solar cell; aging test; multi-environmental coupling; long-term reliability

1. Introduction

Among the various photovoltaic technologies, crystalline silicon solar cells are currently the most mature and widely deployed, accounting for more than 98% of the photovoltaic market share [1]. They are expected to maintain their dominant position for a considerable period in the future [2–4]. Among them, silicon heterojunction (SHJ) solar cells exhibit excellent surface passivation properties and low dark saturation current density (J_0) [5,6]. These

Copyright: © 2026 by the authors. This is an open access article under the terms and conditions of the Creative Commons Attribution (CC BY) license (https://creativecommons.org/licenses/by/4.0/).
Publisher's Note: Scilight stays neutral with regard to jurisdictional claims in published maps and institutional affiliations.

properties enable SHJ solar cells to achieve the highest efficiency theoretically. They also have the advantages of low temperature coefficients and low manufacturing temperatures. However, when SHJ solar cells face the influence of multiple environmental factors, including prolonged exposure to temperature variations, humidity, ultraviolet radiation, acidic substances, and ions under natural operating conditions, the operation lifetime of SHJ solar cell is significantly shortened [7–13]. Therefore, in the process of moving towards large-scale application of PV power generation, in addition to focusing on updating the cell technology to enhance the power of PV modules, efforts need to be made to ensure the long-term stability of PV modules over a 25-year working life [14–16].

Currently, there have been numerous studies on the UV-induced degradation or the impact of DH on SHJ solar cells and modules [17–22], and there are relevant standards such as IEC 61215. However, existing standards and studies usually focus on a single environmental factor. In actual operation, modules are applied in various climatic conditions [23–25], such as deserts, alpine and high-altitude areas, high-heat and high-humidity regions, exposing them to numerous environmental factors [26,27]. The coupling effect of factors like temperature, UV radiation, and high humidity may have different influence mechanisms on SHJ solar cells and modules, making it of great necessity to study the coupling impact of multiple environmental factors [28–30].

Therefore, this paper investigated the performance influence mechanisms of SHJ modules and encapsulants under multi-environmental coupling. Different from traditional single or sequential aging test standards for modules, this study innovatively integrates multiple environmental stresses in experiments to reproduce the real outdoor environment to the greatest extent, and conducts in-depth research on the failure behaviors of encapsulant films under complex environments. This paper can provide support for the adaptation of products for different regions and serves as a key reliability verification link connecting research and development, mass production, and application.

2. Methods and Experimental Details

2.1. Modules Preparation Based on Different Encapsulant Films

The SHJ solar cells used in this paper have a size of M2 (156.75 × 156.75 mm^2), fabricated on n-type monocrystalline silicon wafers with a resistivity of 1.0 Ω·cm. We selected three types of encapsulant films as the encapsulant materials for the modules [31–33]: high-transmittance EVA, high-transmittance POE and light-downshifting EVA. Specially, light-downshifting EVA could convert high-energy ultraviolet light into low-energy visible light. SHJ solar cells were encapsulated into double-glass modules following the structure of glass/encapsulant/cell/encapsulant/glass (Figure 1). Subsequently, to facilitate the direct analysis of the encapsulant films, each type of encapsulant film was separately laminated to induce crosslinking. The lamination parameters are listed in Table S1.

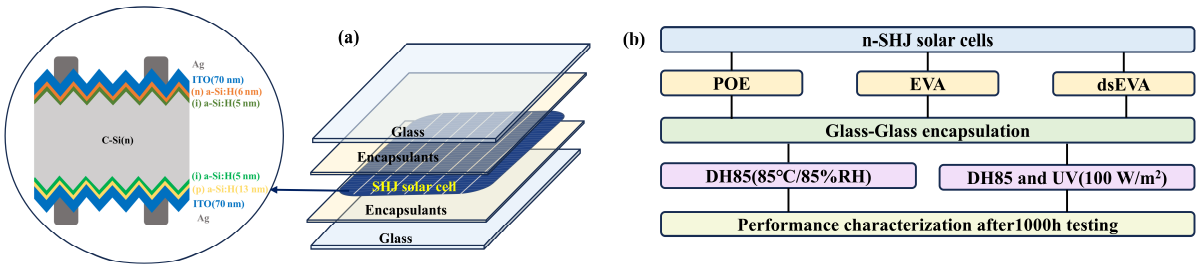


Figure 1. (**a**) The module configuration and schematic of the SHJ cell structure. (**b**) Experimental flow diagrams of the module.

2.2. Accelerated Aging Test and Sample Characterization

All the modules and the laminated encapsulant films that we prepared were placed together in a steady-state environmental aging chamber, to subject UVDH aging experiment. The ultraviolet radiation spectrum used in this experiment covers the range of 280–400 nm (including the UVA and UVB bands), with an irradiance of 100 W/m^2. The total test duration was 1000 h, with measurements performed at intervals of 100 h.

Testing and analyzing of encapsulant films by Fourier Infrared (Thermo Fisher, Waltham, MA, USA), Electronic Universal Material Testing Machine (AG-50KNXPLIS, Shimadzu, Kyoto, Japan), UV-Vis Spectrophotometer (UV-3600, Shimadzu, Kyoto, Japan) and other instruments. For modules, the electrical performance was obtained by the Solar Cell Test System (WaveLabs SINUS 220, Berlin, Germany), including open-circuit voltage (V_{OC}), fill factor (*FF*), short-circuit current (I_{SC}), and conversion efficiency (*PCE*). Meanwhile, the internal defects of the modules were observed through electroluminescence (EL) imaging.

3. Results and Discussion

3.1. The Failure Analysis of Different Encapsulant Films

Optical and Barrier Properties Characterization**.** Figure 2a shows the average transmittance of EVA encapsulant film fall by 5.08% and 5.28% after 1000h of DH and UVDH test, respectively. Similarly, the average transmittance of POE film was reduced by 1.93% and 3.7% in the two tests, respectively. According to the change of transmittance in short wavelength band, it can be seen that POE has better anti-aging ability in short wavelength band compared with EVA (Figure S1). It is worth noting that, under UVDH conditions, the average transmittance of the dsEVA encapsulant film increased by 0.89%, primarily reflected in a 19.72% increase in short-wavelength transmittance. This may be attributed to the degradation of the light-shifting particles during aging, leading to the failure of their ultraviolet-to-blue conversion function. Consequently, more short-wavelength light penetrates the film, resulting in an abnormal increase in transmittance.

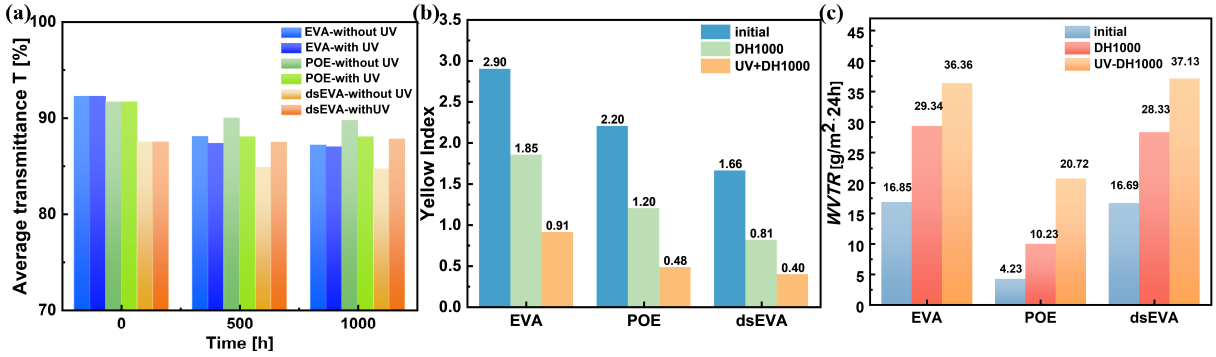


Figure 2. Comparison of three encapsulant films before and after aging. (**a**) Average optical transmittance. (**b**) Change in Yellowness Index (ΔYI). (**c**) Water vapor transmission rate.

Given that the reduction in optical transmittance is strongly linked to yellowing, the chromaticity of the three encapsulant films was measured before and after the aging process. In this paper, a low index corresponds to the reference yellowing state, indicating material degradation; a high index signifies that the sample deviates from the yellowing trend with superior aging stability. The lower of index, the closer the sample is to the reference yellowing state, while the higher of index, the larger the color difference from the reference yellow. As shown in Figure 2b, the yellow index of all three films decreased after aging, demonstrating that the films gradually approach the reference yellowing state and undergo degradation-induced yellowing. This phenomenon can be attributed to a degradation reaction of the encapsulant film under the synergistic effects of light, heat, oxygen, and moisture, leading to the formation of conjugated polyene chromophores [34,35].

We further observed the changes in water vapor transmission rate (WVTR) of encapsulant films. As shown in Figure 2c, with the progression of aging, the WVTR of three encapsulant films increased significantly, and the UVDH group exhibited higher WVTR than the DH group. This indicates that additional UV irradiation causes significant changes in the network structure density of the encapsulant, making it easier for water molecules to pass through. Specifically, UV irradiation leads to the breaking of chemical bonds in the encapsulant, damaging the molecular chain structure of the encapsulant films [36]. For EVA materials, UV irradiation accelerates the degradation and decomposition of VA units, leading to changes in crosslinking density and an increase in molecular chain scission [37]. Consequently, the encapsulant becomes looser and more brittle, reducing its ability to shield moisture. Furthermore, as shown in Figure S2, the bulk resistivity of the three types of encapsulant films decreased significantly under both DH and UVDH aging tests, indicating that these films have become less capable of hindering ion migration from the glass to the cell surface.

Mechanical Properties Testing. The peel strength value characterizes the adhesion between the encapsulant and cell, as well as between the encapsulant and glass. In the specific tests, we measured the peel strength at the encapsulant/cell interface and the encapsulant/glass interface, respectively. A higher peeling strength can extend the outdoor service life of modules. As shown in Figure 3, the initial peeling strength between POE and the cell is lower than that of EVA film, which is caused by the weaker intermolecular forces of POE as a non-polar material. After DH and UVDH aging test, the peeling strength of the three encapsulant films decreases significantly, with POE film showing the most severe degradation. Figures S3 and S4 similarly show the significant decrease in elongation at break and tensile strength of the three encapsulant films after UVDH aging. These results indicate that after DH and UVDH aging, the molecular chains of the encapsulant films break, leading to a reduction in molecular weight, which in turn causes significant degradation of mechanical properties.

In summary, the decline in mechanical properties of the encapsulant will directly weaken its protective effect on the cell. A reduction in elastic modulus diminishes the film's stress-buffering capacity, thereby increasing the mechanical stress transferred to the solar cells and elevating the risk of microcracking. Meanwhile, weakened interfacial adhesion promotes delamination and moisture ingress, which can trigger corrosion and potential-induced degradation (PID) [38]. All of these factors degrade the structural integrity of module, accelerate power loss and seriously shortening the lifespan of the module.

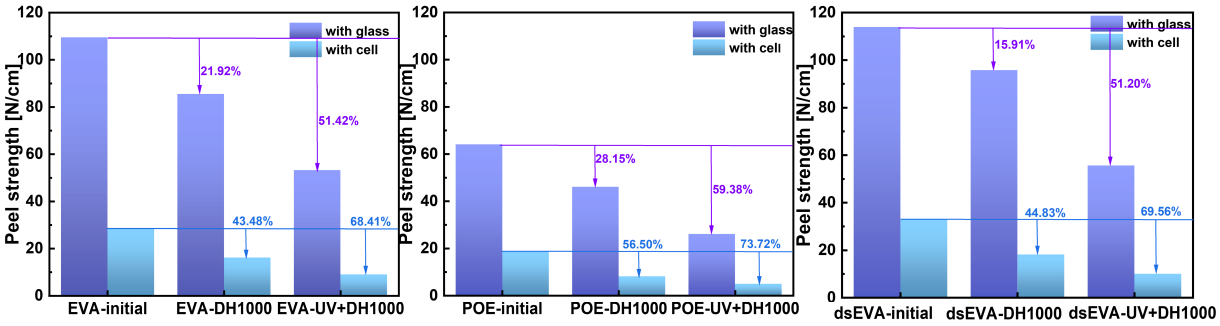


Figure 3. Changes in peeling strength with SHJ solar cells/glass of the three types of encapsulant films before and after aging.

Chemical Characterization. From bottom to top, Figure 4 shows the infrared spectra of EVA, dsEVA, and POE encapsulant films. The characteristic peaks of C-H are at 2920 cm^{-1} and 2853 cm^{-1}. The characteristic peaks of EVA include those of vinyl acetate (VA) at 1735, 1242, and 1021 cm^{-1}, as well as those of ethylene at 2920, 2853, 1465, and 1731 cm^{-1}. The presence of carbonyl groups (C=O, 1740 cm^{-1}) in VA units indicates that EVA is a polar compound. Ethers are directly linked to the polymer backbone as part of it, making EVA more prone to deacetylation reactions. The decrease in the intensity of the carbonyl (C=O) absorption peak near 1700 cm^{-1} suggests that oxidation reactions occur in the encapsulant film during the aging test. Free-radical chain reactions lead to the breaking of molecular chains in the film and the generation of numerous carbonyl groups. The VA units in EVA film are sensitive to UV light, making them prone to decomposition and formation of carbonyl groups. Although POE film exhibits better oxidation resistance, it still shows significant generation of carbonyl groups under damp-heat environment, indicating that its anti-aging capability remains limited under extreme conditions. In the range of 1100–1300 cm^{-1}, the absorption peaks related to C-O stretching vibrations have shown obvious changes, especially in EVA films. Such changes indicate that ester groups undergo degradation or chemical rearrangement, which may reduce the mechanical and encapsulant properties of the material. In POE films, the C-O-C groups are located outside the main chain skeleton, and the C atoms are covalently bonded to another C atom of the acrylate unit, giving the material a non-polar nature. This hinders deacetylation reactions, and the related group changes are also insignificant.

3.2. The Degradation Analysis of Silicon Heterojunction Modules

To compare the UVDH and standard DH aging tests for modules, this paper shows the electrical performance degradation of three encapsulant-based modules after 1000 h aging in two environments. Figure 5a shows that the modules encapsulated with three types of films exhibit greater electrical performance degradation under UVDH environment. This indicates that the UVDH is a more severe reliability challenge for PV modules than the conventional DH test. Given the current attenuation, we performed EQE tests on the three modules before and after aging to assess spectral response and current loss in different bands. In Figure 5b, the EQE curves of the three modules all have a large drop in the 0–400 nm band and the 900–1200 nm band, indicating that UVDH aging mainly affects the spectral response capability in short-wavelength and long-wavelength bands. For modules, this is also closely related to the performance of encapsulant films, solder tapes, grid lines, etc.

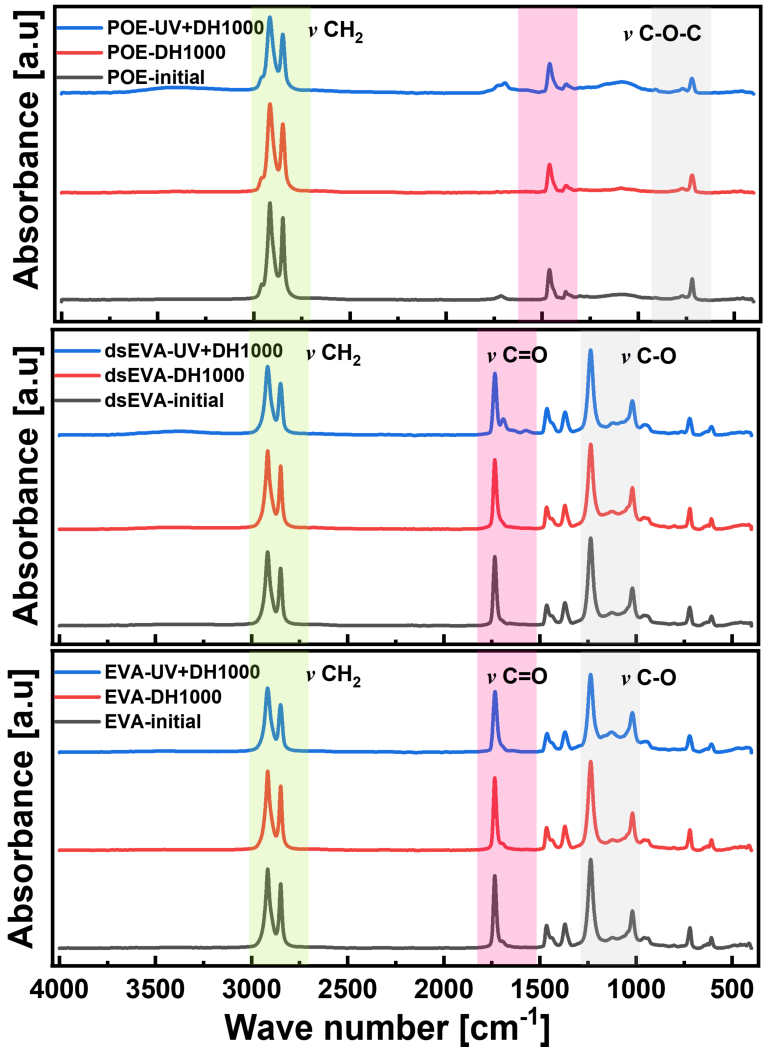


Figure 4. FTIR spectra of three encapsulant films before and after aging test.

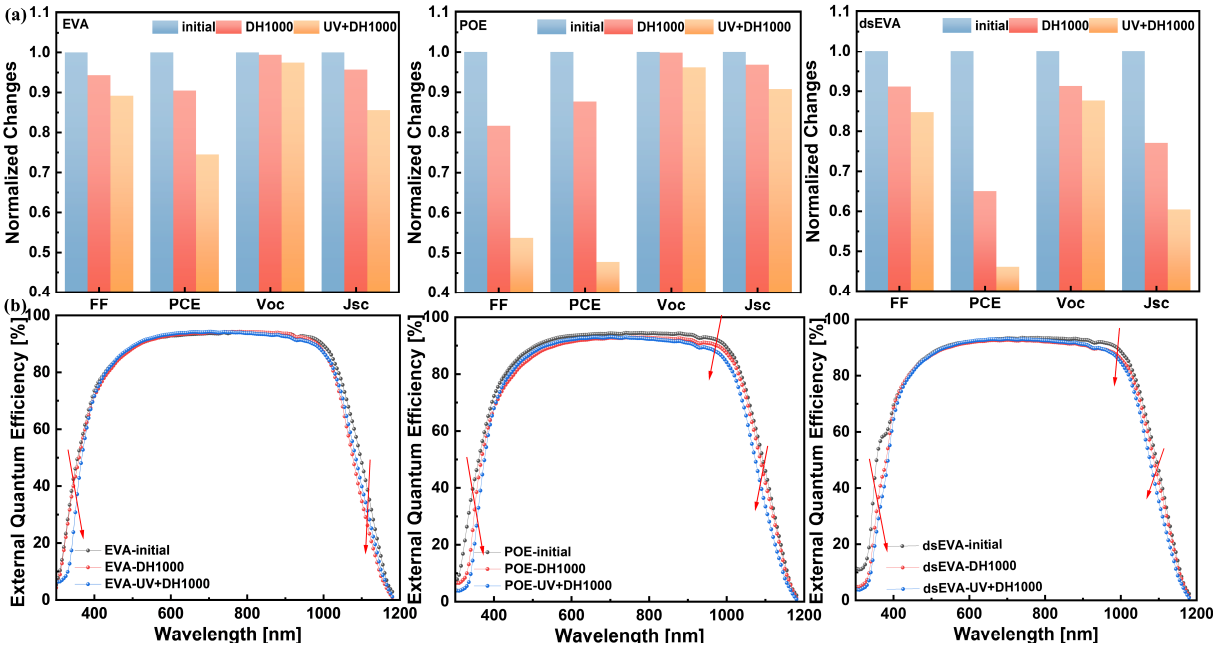


Figure 5. Changes in module performance after DH vs. UVDH. (**a**) Normalized changes in electrical performance. (**b**) Comparison of EQE curves of SHJ modules captured before and after 1000 h of aging test.

The aging status of the modules was monitored by EL imaging. In Figure 6, for EVA-encapsulated modules, the bright regions in EL images gradually diminished starting at 400 h, accompanied by darkening areas spreading

from the edges toward the center. This darkening effect was more pronounced under UVDH conditions, with significantly larger affected areas. This indicates that in damp-heat environment, as glass is essentially impermeable to water, water vapor gradually infiltrates from the module edges toward the center. The hydrolysis of EVA produces acetic acid, which corrodes the SHJ cells, increasing contact resistance and gradually deteriorating surface passivation and p-n junction quality. The EL images of the POE-encapsulated module are quite different, showing the gradual appearance and deepening of stripe-like dark spots. Similarly, the bright regions in the EL images diminish, with more dark spots spreading inward from the edges. This is primarily due to the inherently lower adhesion strength at the interface between the POE encapsulant film and SHJ cells. Under prolonged DH exposure, the adhesion gradually weakens, leading to delamination between the encapsulant and cells. This results in poor contact between the solder ribbons and grid lines, increasing (series resistance) R_s and causing a sharp decline in *FF*. This is especially true in modules subjected to UVDH conditions, where adhesion strength is further weakened. The dsEVA-encapsulated module, exhibits similar degradation to the EVA module, but more pronounced. Brightness gradually weakened, and the blackened area increased until eventual total blackening, which indicates severe deterioration of the passivation effect. At the same time, a large amount of acetic acid produced by the hydrolysis will cause corrosion of the cell, grid lines, and welding tape, resulting in poor electrode contact and further electrical performance loss.

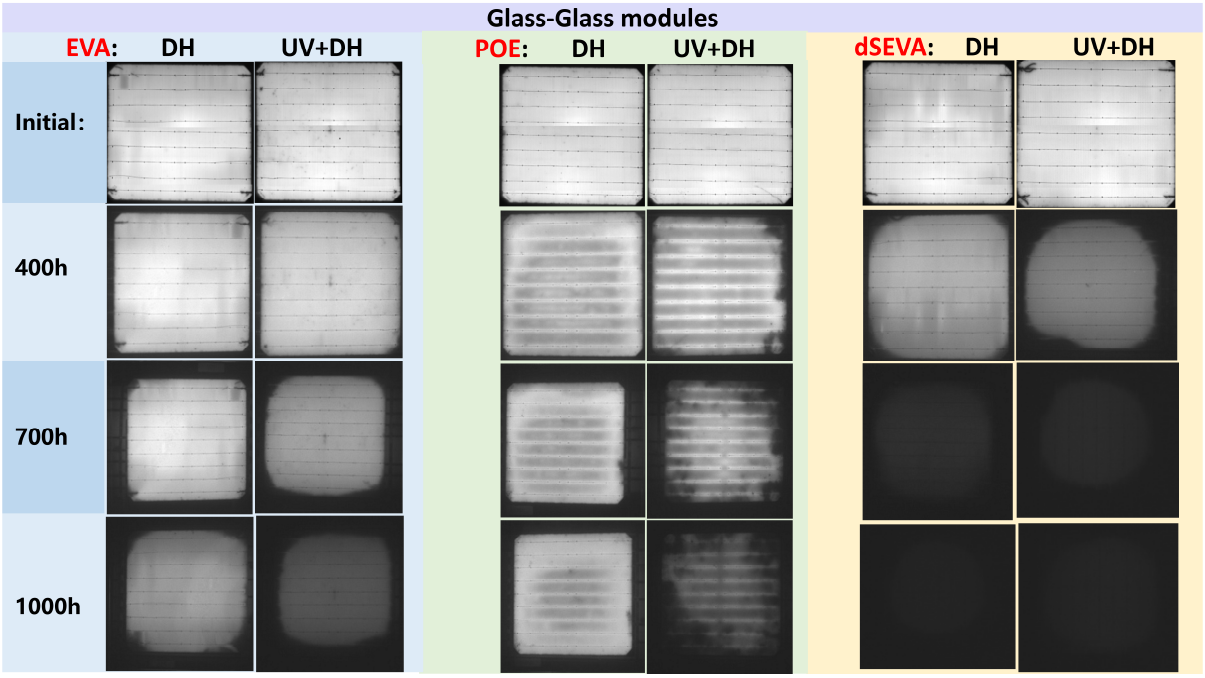


Figure 6. The EL images of modules after 1000 h DH and UVDH aging test.

3.3. Innovation of Encapsulant Materials under Multi-Factor Coupling

To address UV-induced degradation, current encapsulant films often adopt strategies such as photoconversion or UV blocking. However, this study found that under the coupled UV and DH effects, the light-downshifting EVA encapsulant film failed to converts UV to blue light. It is speculated that this is related to the failure of the light-downshifting agent in the DH environment, and this can be verified by the increased transmittance of the photoconversion EVA in the 300–400 nm wavelength range (Figure S1). Therefore, while considering the impact of UV light, more attention should be paid to optimizing encapsulant materials under synergistic multiple factors to improve the weather resistance of PV modules in practice.

Taking the coupled UVDH effects as an example, weather-resistant encapsulants must possess excellent UV and DH resistance: they should inhibit UV-induced aging and power loss while blocking moisture to ensure long-term sealing and cell stability. Currently, a relatively direct approach is to develop new encapsulant systems by composing and optimizing existing UV-resistant and damp-heat-resistant materials. For instance, conventional photoconversion EVA is prone to hydrolysis in the damp-heat environment, leading to the failure of the light-downshifting agent. Thus, it is feasible to use POE or TOP materials in combination with the light-downshifting agent, which have better water resistance [5,39–41]. Based on the comparative results of this study, it is speculated that combining photoluminescent down-conversion functionality with a POE matrix may lead to superior anti-aging

performance under UVDH coupled conditions. Subsequent work will systematically verify this hypothesis [42]. In addition, research on coated glass under single UV or DH conditions is relatively sufficient, but studies under coupled effects remain insufficient. It is necessary to introduce a double-layer coating structure: a dense and inert silicon dioxide barrier layer on the inner side of the glass, while an anti-reflective coating layer doped with rare earth-based UV blockers on the outer side (Figure S5). This structure can not only convert UV light into visible light to delay aging, but also effectively inhibit moisture intrusion and sodium ion migration, thereby improving the anti-aging performance of the module.

4. Conclusions

This study compares DH and UVDH coupled aging tests to simulate the failure behavior of photovoltaic modules under multi-factor synergistic outdoor conditions. After 1000 h of aging tests, the results reveal that ultraviolet radiation accelerates the degradation of the encapsulant films initially induced by DH under combined DH and UV exposure, thereby significantly affecting the power generation efficiency of the modules. Accordingly, it is recommended that multi-factor coupled aging tests be integrated into the reliability evaluation system to precisely predict the long-term performance and service lifetime of photovoltaic modules under practical service conditions. Based on the present findings, future research will focus on mechanistic explorations including the evolution of cell interface states and degradation kinetics of encapsulant materials. Such further studies aim to uncover the intrinsic failure mechanism under multi-stress coupled aging and provide universal theoretical guidance for relevant research fields.

Supplementary Materials

The additional data and information can be downloaded at: https://media.sciltp.com/articles/others/260717 0900297168/MM-26050055-SM.pdf. Table S1: The lamination process parameters; Figure S1: Changes in optical properties of three types of encapsulant films before and after aging. (a) Transmittance. (b) Reflectance; Figure S2: Changes in bulk resistivity of the three types of encapsulant films before and after aging; Figure S3: Changes in elongation at break of the three types of encapsulant films before and after aging; Figure S4: Changes in tensile strength of the three types of encapsulant films before and after aging; Figure S5: Optimization of encapsulant materials: bilayer coating glass and light-downshifting encapsulant film with low WVTR.

Author Contributions

H.L.: Writing—review & editing, Data curation, Visualization. Y.H.: Formal analysis, Funding acquisition, Project administration, Resources. Q.D.: Writing—original draft, Formal analysis, Conceptualization. X.Y.: Resources, Investigation. Y.Z.: Resources, Project administration, Investigation. C.H.: Resources, Conceptualization, Investigation. T.C.: Supervision, Resources, Funding acquisition, Project administration, Investigation, Conceptualization. L.L.: Supervision, Resources, Investigation, Conceptualization. W.L.: Supervision, Resources, Conceptualization, Funding acquisition, Project administration. J.Y.: Writing review & editing, Writing—original draft, Software, Resources, Project administration, Investigation, Funding acquisition, Conceptualization. All authors have read and agreed to the published version of the manuscript.

Funding

This research was financially supported by Sichuan Science and Technology Program (2025YFCY0011), Chengdu Science and Technology Program (2025-GH02-00012-HZ) and Leshan West Silicon Materials Photovoltaic New Energy Industry Technology Research Institute (2024GYKF1) (J.Y.); Key Research Project of Zhejiang Province (No. 2025C01142) (T.C.); National Natural Science Foundation of China (grant nos. T2322028, 62474184), the CAS Project for Young Scientists in Basic Research (grant no. YSBR-102), the Talent Plan of Shanghai Branch, Chinese Academy of Sciences (grant no. CASSHBQNPD-202-001) (W.L.).

Institutional Review Board Statement

Not applicable.

Informed Consent Statement

Not applicable.

Data Availability Statement

Data are available from the corresponding authors upon reasonable request.

Conflicts of Interest

The authors declare no conflict of interest.

Use of AI and AI-Assisted Technologies

No AI tools were utilized for this paper.

References

1. Photovoltaics Equipment. *International Technology Roadmap for Photovoltaic (ITRPV): 2024 Results*, 16th ed.; VDMA: Frankfurt/Main, Germany, 2025. Available online: https://www.vdma.eu/de/international-technology-roadmap-photovoltaic (accessed on 7 May 2026).
2. Addonizio, M.; Antonaia, A. Textured p-type crystalline silicon surfaces obtained by multi-step plasma process for SHJ solar cells. *Vacuum* **2023**, *215*, 112284. https://doi.org/10.1016/j.vacuum.2023.112284.
3. Andreani, L.C.; Bozzola, A.; Kowalczewski, P.; et al. Silicon solar cells: Toward the efficiency limits. *Adv. Phys.-X* **2019**, *4*, 1548305. https://doi.org/10.1080/23746149.2018.1548305.
4. Bashiri, H.; Karami, M.A.; Nejad, S.M. An analytical approach for modeling of high-efficiency crystalline silicon solar cells with homo–hetero junctions. *Mater. Sci. Semicond. Process* **2020**, *111*, 104960. https://doi.org/10.1016/j.mssp.2020.104960.
5. Bai, Y.; Zhao, Y.; Li, J.; et al. Lower levelized cost of energy achievement of silicon heterojunction solar modules with low water vapor transmission rate encapsulants. *Energy Technol.* **2023**, *11*, 2201466. https://doi.org/10.1002/ente.202201466.
6. Green, M.A.; Dunlop, E.D.; Yoshita, M.; et al. Solar cell efficiency tables (version 66). *Prog. Photovolt.* **2025**, *33*, 795–810. https://doi.org/10.1002/pip.3919.
7. Arriaga Arruti, O.; Gnocchi, L.; Jeangros, Q.; et al. Potential-induced degradation in bifacial silicon heterojunction solar modules: Insights and mitigation strategies. *Prog. Photovolt.* **2024**, *32*, 304–316. https://doi.org/10.1002/pip.3765.
8. Li, X.; Yang, Y.; Jiang, K.; et al. Potential-free sodium-induced degradation of silicon heterojunction solar cells. *Prog. Photovolt.* **2023**, *31*, 939–948. https://doi.org/10.1002/pip.3698.
9. Ye, H.; Huang, S.; Qian, C.; et al. Short wavelength photons destroying Si-H bonds and its influence on high-efficiency silicon solar cells and modules. *Sol. RRL* **2023**, *7*, 2300334. https://doi.org/10.1002/solr.202300334.
10. Sen, C.; Wang, H.; Wu, X.; et al. Four failure modes in silicon heterojunction glass-backsheet modules. *Sol. Energy Mater. Sol. Cells* **2023**, *257*, 112358. https://doi.org/10.1016/j.solmat.2023.112358.
11. Yu, J.; Bai, Y.; Qiu, Q.; et al. Reliability of transparent conductive oxide in ambient acid and implications for silicon solar cells. *eScience* **2024**, *4*, 100241. https://doi.org/10.1016/j.esci.2024.100241.
12. Deng, Q.; Ye, H.; Huang, S.; et al. Mechanism of photon-induced performance changes in silicon heterojunction solar cells. *Sci. China-Mater.* **2024**, *67*, 2873–2879. https://doi.org/10.1007/s40843-024-2997-7.
13. Bai, Y.; Zhang, Y.; Luo, H.; et al. Degradation-free high-efficiency fluoride-coating solar cells via precision interface engineering. *Prog. Photovolt.* **2025**, *33*, 1260–1270. https://doi.org/10.1002/pip.70018.
14. Damo, U.; Ozoegwu, C.G.; Ogbonnaya, C.; et al. Effects of light, heat and relative humidity on the accelerated testing of photovoltaic degradation using Arrhenius model. *Sol. Energy* **2023**, *250*, 335–346. https://doi.org/10.1016/j.solener.2023.01.002.
15. Gaddam, S.K.; Pothu, R.; Boddula, R. Advanced polymer encapsulates for photovoltaic devices—A review. *J. Materiomics* **2021**, *7*, 920–928. https://doi.org/10.1016/j.jmat.2021.04.004.
16. Meena, R.; Pareek, A.; Gupta, R. A comprehensive Review on interfacial delamination in photovoltaic modules. *Renew. Sust. Energy Rev.* **2024**, *189*, 113944. https://doi.org/10.1016/j.rser.2023.113944.
17. Ren, J.; Zhao, W.; Shi, J.; et al. Predicting the lifetime of HJT modules towards the outdoor real-world environment. *Sol. Energy Mater. Sol. Cells* **2024**, *272*, 112885. https://doi.org/10.1016/j.solmat.2024.112885.
18. Razzaq, S.; Wei, L.; Jiao, R.; et al. Enhancing UV light stability in commercial silicon HJT solar cells and modules. *Sol. Energy* **2025**, *298*, 113735. https://doi.org/10.1016/j.solener.2025.113735.
19. Liu, W.; Zhang, L.; Yang, X.; et al. Damp-heat-stable, high-efficiency, industrial-size silicon heterojunction solar cells. *Joule* **2020**, *4*, 913–927. https://doi.org/10.1016/j.joule.2020.03.003.
20. Park, H.; Jeong, J.; Shin, E.; et al. A reliability study of silicon heterojunction photovoltaic modules exposed to damp heat testing. *Microelectron. Eng.* **2019**, *216*, 111081. https://doi.org/10.1016/j.mee.2019.111081.
21. Segbefia, O.K.; Imenes, A.G.; Saetre, T.O. Moisture ingress in photovoltaic modules: A review. *Sol. Energy* **2021**, *224*, 889–906. https://doi.org/10.1016/j.solener.2021.06.055.
22. Zeng, F.; He, Y.; Xu, S.; et al. Accelerated degradation of PET-based photovoltaic backsheets under UV and acetic acid

exposure. *Polymer* **2024**, *312*, 127671. https://doi.org/10.1016/j.polymer.2024.127671.
23. Kivambe, M.; Abdallah, A.; Figgis, B.; et al. Comprehensive assessment of performance and reliability of PERC, TOPCon and SHJ modules in desert climates. *Sol. Energy* **2025**, *295*, 113555. https://doi.org/10.1016/j.solener.2025.113555.
24. Frischholz, Y.; Schilt, U.; Sharma, V.; et al. Confirmation of the power gain for solar photovoltaic systems in alpine areas and across scales. *Front. Energy Res.* **2024**, *12*, 1372680. https://doi.org/10.3389/fenrg.2024.1372680.
25. Tsuchida, S.; Tsuno, Y.; Sato, D.; et al. Power generation characteristics of vertical bifacial photovoltaic arrays in heavy snow regions. *EPJ Photovolt.* **2024**, *15*, 32. https://doi.org/10.1051/epjpv/2024029.
26. Barretta, C.; Macher, A.E.; Ascencio-Vásquez, J.; et al. Degradation of crystalline silicon photovoltaic modules installed in different climates. In Proceedings of the 2022 IEEE 49th Photovoltaics Specialists Conference (PVSC), Philadelphia, PA, USA, 5–10 June 2022; pp. 0680–0682. https://doi.org/10.1109/PVSC48317.2022.9938590.
27. Santhakumari, M.; Sagar, N. A review of the environmental factors degrading the performance of silicon wafer-based photovoltaic modules: Failure detection methods and essential mitigation techniques. *Renew. Sust. Energy Rev.* **2019**, *110*, 83–100. https://doi.org/10.1016/j.rser.2019.04.024.
28. Tsanakas, J.; Babics, M.; Mezzasalma, F.; et al. Long-term field degradation of crystalline-silicon PV modules: Insights from fifteen years of monitoring and forensic analysis. *EPJ Photovolt.* **2026**, *17*, 14. https://doi.org/10.1051/epjpv/2026006.
29. Uličná, S.; Sinha, A.; Miller, D.C.; et al. PV encapsulant formulations and stress test conditions influence dominant degradation mechanisms. *Sol. Energy Mater. Sol. Cells* **2023**, *255*, 112319. https://doi.org/10.1016/j.solmat.2023.112319.
30. Liu, K.; Miller, D.C.; Bosco, N.; et al. Advancing steady-state and sequenced accelerated aging for assessing the adhesion degradation of contemporary encapsulants. In Proceedings of the 2025 IEEE 53rd Photovoltaic Specialists Conference (PVSC), Montreal, QC, Canada, 8–13 June 2025; pp. 0738–0743. https://doi.org/10.1109/PVSC59419.2025.11133400.
31. Säckl, G.; Wallner, G.M.; Duchoslav, J.; et al. Advanced analysis of ethylene vinyl acetate copolymer materials for photovoltaic modules. *Polym. Test* **2024**, *132*, 108381. https://doi.org/10.1016/j.polymertesting.2024.108381.
32. Lee, K.; Kim, D.; Kim, S.H.; et al. Improving the physical properties of polyolefin elastomer encapsulants by radical initiators for reliable photovoltaic modules. *Polym. Test* **2025**, *151*, 108954. https://doi.org/10.1016/j.polymertesting.2025.108954.
33. Sun, Z.; Xia, Z.; Yan, D.; et al. Industrial-scale silicon heterojunction photovoltaic module towards 25% efficiency enabled by high-quantum-yield $CaSrSiO_4$: Ce^{3+} inorganic downshifting materials. *Prog. Photovolt.* **2025**, *33*, 678–688. https://doi.org/10.1002/pip.3908.
34. Pern, F.; Czanderna, A.; Emery, K.; et al. Weathering degradation of EVA encapsulant and the effect of its yellowing on solar cell efficiency. In Proceedings of the The Conference Record of the Twenty-Second IEEE Photovoltaic Specialists Conference-1991, Las Vegas, NV, USA, 7–11 October 1991; pp. 557–561. https://doi.org/10.1109/PVSC.1991.169275.
35. Pern, F.; Czanderna, A. Characterization of ethylene vinyl acetate (EVA) encapsulant: Effects of thermal processing and weathering degradation on its discoloration. *Sol. Energy Mater. Sol. Cells* **1992**, *25*, 3–23. https://doi.org/10.1016/0927-0248(92)90013-F.
36. Fiandra, V.; Sannino, L.; Andreozzi, C.; et al. New PV encapsulants: Assessment of change in optical and thermal properties and chemical degradation after UV aging. *Polym. Degrad. Stab.* **2024**, *220*, 110643. https://doi.org/10.1016/j.polymdegradstab.2023.110643.
37. Jin, J.; Chen, S.; Zhang, J. UV aging behaviour of ethylene-vinyl acetate copolymers (EVA) with different vinyl acetate contents. *Polym. Degrad. Stab.* **2010**, *95*, 725–732. https://doi.org/10.1016/j.polymdegradstab.2010.02.020.
38. Hasan, A.A.; Ahmed Alkahtani, A.; Shahahmadi, S.A.; et al. Delamination-and electromigration-related failures in solar panels—A review. *Sustainability* **2021**, *13*, 6882. https://doi.org/10.3390/su13126882.
39. Barretta, C.; Oreski, G.; Feldbacher, S.; et al. Comparison of degradation behavior of newly developed encapsulation materials for photovoltaic applications under different artificial ageing tests. *Polymers* **2021**, *13*, 271. https://doi.org/10.3390/polym13020271.
40. Adothu, B.; Bhatt, P.; Chattopadhyay, S.; et al. Newly developed thermoplastic polyolefin encapsulant–A potential candidate for crystalline silicon photovoltaic modules encapsulation. *Sol. Energy* **2019**, *194*, 581–588. https://doi.org/10.1016/j.solener.2019.11.018.
41. Hou, J.; Ma, D.; Zhang, Z.; et al. Visible-light-driven Fe-catalyzed alkylation for synthesizing functionalized polyolefin elastomers as advanced encapsulants in photovoltaic modules. *React. Funct. Polym.* **2024**, *205*, 106072. https://doi.org/10.1016/j.reactfunctpolym.2024.106072.
42. Xie, N.; Zhang, Y.; Wang, S.; et al. Encapsulation Films for Silicon Solar Cells: Multifunctional Polyolefin Elastomeric Films Fabricated by *In Situ* Grafting a Eu^{3+} Complex. *ACS Appl. Polym. Mater.* **2025**, *7*, 5573–5583. https://doi.org/10.1021/acsapm.5c00455.